Nano Energy (2015) 11, 481–489

Available online at www.sciencedirect.com

ScienceDirect

journal homepage: www.elsevier.com/locate/nanoenergy

RAPID COMMUNICATION

Graphdiyne for high capacity and long-life lithium storage

Changshui Huang[a,b,1], Shengliang Zhang[b,c,1], Huibiao Liu[a], Yongjun Li[a], Guanglei Cui[b], Yuliang Li[a,*]

[a]Beijing National Laboratory for Molecular Sciences (BNLMS), CAS Key Laboratory of Organic Solids, Institute of Chemistry, Chinese Academy of Sciences, Beijing 100190, P.R.China
[b]Qingdao Institute of Bioenergy and Bioprocess Technology, Chinese Academy of Sciences, Qingdao, 266101, P.R. China
[c]Graduate University of Chinese Academy of Sciences, Beijing 100190, P.R. China

Received 16 October 2014; received in revised form 13 November 2014; accepted 13 November 2014
Available online 21 November 2014

KEYWORDS
Graphdiyne;
Electrochemical performance;
Lithium storage;
High capacity;
Long cycle lives

Abstract
There is an increasing demand for improvement of the capacity, rate performance, and life cycle of lithium-ion batteries to meet the requirements of low-emission vehicles, such as hybrid electric and plug-in hybrid electric vehicles. In this article, we report the application of graphdiyne (GDY) as high efficiency lithium storage materials and elucidate the method of lithium storage in multilayer GDY. GDY is a novel carbon allotrope comprising sp- and sp^2-hybridized carbon atoms. Lithium-ion batteries featuring GDY-based electrode exhibit excellent electrochemical performance, including high specific capacities, outstanding rate performances, and a long cycle lives. We obtained reversible capacities of up to 520 mAh/g after 400 cycles at a current density of 500 mA/g. At an even higher current density of 2 A/g, cells incorporating GDY-based electrodes retained a high specific capacity of 420 mAh/g after 1000 cycles.

Introduction

Carbon-based materials are being heavily investigated for their applications as next-generation lithium (Li) storage materials [1-5]. Because of its low cost and high chemical stability, graphite is the most commonly used anode material in commercialized batteries [6]. Nevertheless, its limited Li storage capacity (372 mAh/g, LiC_6) and structural disorder upon prolonged cycling prevent graphite from meeting the increasing demand for Li-ion batteries in the modern world. In the pursuit of higher capacity, rate capability and longer cycling life, other carbon structures have been studied, including fullerenes [7-9], carbon nanotubes (CNTs) [10-13],

*Corresponding author.
E-mail address: ylli@iccas.ac.cn (Y. Li).
[1]These authors contributed equally to this work.

http://dx.doi.org/10.1016/j.nanoen.2014.11.036
2211-2855/

and graphene [14–17]. The carbon atoms in these structures are all sp^2-hybridized, the same as those in graphite. Although the Li capacity can be improved greatly with these different dimensionalities and morphologies, the nature of the Li-intercalated layer does not change significantly when compared to graphite. Graphdiyne (GDY) is a new carbon allotrope that was only synthesized recently [18,19]. GDY is composed of sp^2- and sp-hybridized carbon atoms and is predicted to be the most stable of the various diacetylenic non-natural carbon allotropes. Wang and colleagues confirmed the electronic structure and solid-state structure of GDY determined using X-ray absorption spectroscopy and scanning transmission X-ray microscopy [20].GDY and its unusual structure promises to yield new functional materials displaying novel and enhanced properties. GDY is a 2D, one-atom thick layer of strongly bonded carbon atoms that exhibit chemical stability and electrical conductivity [18,19].Unlike wholly sp^2-hybridized carbon structures, the flat carbon (sp^2 and sp) network endows the GDY material with uniformly distributed pores, and tunable electronic properties. GDY has been predicted to have promising applications as a Li storage material in batteries due to its high capacity and rate capability [20–26]. Here, we are showing that GDY films exhibited a high specific Li capacity, long cycle life, and high stability as electrode materials in Li-ion batteries. The reversible capacities of GDY films are up to 520 mAh/g after 400 cycles at a current density of 500 mA/g and the cells incorporating GDY-based electrodes retained a high specific capacity of 420 mAh/g after 1000 cycles at an even higher current density of 2 A/g.

The structure of GDY is related to that of graphene, but with the introduction of butadiynelinkages ($-C\equiv C-C\equiv C-$) to form 18-C hexagons (Fig. 1). With regard to applications in Li storage, many theoretical studies, using density functional theory [24] and first-principles calculations [21,25], have determined the absorption and diffusion of Li atoms within GDY. High-capacity Li storage in the form of LiC_3 (744 mAh/g) has been predicted—twice the specific capacity of graphite. The unique atomic arrangement and electronic structure of GDY enable Li atoms to diffuse readily upon a GDY layer with moderate energy barriers ranging from 0.18 to 0.84 eV. Compared with graphene, the 18-C hexagon structure of GDY results in a lower atom density and, accordingly, a larger specific surface area. Taken together, all of these features suggest that GDY has the potential to ensure efficient Li storage.

In this study, we demonstrate the application of GDY as an efficient Li storage material for the fabrication of high-performance Li-ion batteries. We achieved a battery exhibiting high specific capacity, an outstanding rate performance, and a superior cycle life through the direct use of GDY fabricated on a copper surface without the addition of any polymer binders or conductive additives. This battery featured a reversible capacity of up to 520 mAh/g after 400 cycles at a current density of 500 mA/g. At an even higher current density of 2 A/g, cells incorporating GDY-based electrodes retained their high specific capacity at 420 mAh/g after 1000 cycles. We elucidate the method behind the Li atom storage in multilayer GDY by using GDY with varying thicknesses. The intercalation of Li atoms occurs primarily through both interlayer insertion/extraction process and surface absorption/desorption process.

Experimental section

Synthesis of GDY films

Copper foil was washed with 4 M hydrochloric acid (HCl) (100 mL), sonicated for 3 min, washed with water and ethanol, sonicated for 3 min, washed twice with acetone, and dried under nitrogen (N_2). Several (10) pieces of copper foil ($2 \times 2\ cm^2$) and pyridine (50 mL) were charged in a three-neck flask; the mixture was heated at 120 °C under N_2 for 1 h and then the temperature was decreased to 80 °C. Hexakis[(trimethylsilyl)ethynyl]benzene (50 mg) was dissolved in tetrahydrofuran (THF) (50 mL) in an ice bath (ice and ammonium

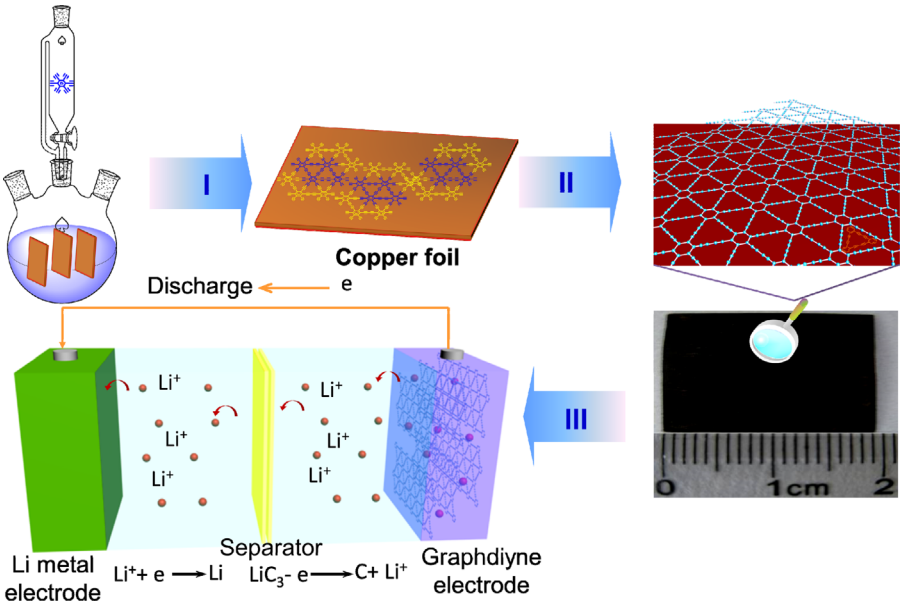

Fig. 1 Schematic of the GDY synthesis and Li-ion batteries preparation process. (I) synthesis schematic of GDY. (II) photograph of GDY sample and Ball-and-stick model of the structure of GDY. (III) representation of an assembled GDY-based battery.

chloride) and purged with N_2 for 30 min. 1 M tetra-n-butylammonium fluoride (TBAF) in THF (2.5 mL)was added under N_2 and then the mixture was stirred for 15 min at this low temperature (generally, the solution should be purple; it is related to the quality of the TBAF solution). The reaction mixture was diluted with ethyl acetate, washed three times with saturated sodium chloride (NaCl), dried magnesium sulfate ($MgSO_4$), and filtered. The solvent was evaporated under vacuum while maintaining the temperature below 30 °C. The deprotected compound should be processed in dark, rapidly, and at low temperature. The residue was dissolved in pyridine (50 mL),transferred to a N_2-protected constant addition funnel, and added dropwise into the mixture containing pyridine (50 mL) and the pieces of copper foil at 80 °C; this addition process lasted for 8 h. The entire process, from deprotection to addition, should be continuous and rapid to avoid contact with oxygen. After addition of the deprotected compound, the reaction mixture was maintained at 120 °C for 3 days. Upon completion of the reaction, the pyridine was evaporated under reduced pressure. A black film was obtained on the copper foil. We carefully scraped the GDY on one side. So the sample we used for test only have GDY left on one side of the copper foil. For purifying the GDY film, the pieces of copper foil were washed sequentially with acetone, hot (80 °C) dimethylformamide (DMF) and ethanol. The copper foil covered GDY film was heated at 100 °C in vacuum for 1 h to get sample GDY-1.

When 100 mg and 150 mg hexakis[(trimethylsilyl)ethynyl] benzene were used, respectively, sample GDY-2 and GDY-3 were prepared.

Electrochemical measurements

The electrochemical experiments were performed in 2032 coin-type cells. The GDY films grown on the copper foil were cut into pieces (0.5 cm × 0.6 cm, 0.3 cm^2), dried in a vacuum oven at 120 °C for 4 h, and then used as working electrodes without adding any binders. Pure Li foil was used as the counter electrode; it was separated from the working electrode by a Celgard 2500 polymeric separator. The electrolyte was1M $LiPF_6$ in EC/DMC (1:1, v/v) or 1M $LiPF_6$ in EC/DMC/DEC (1:1:1, v/v/v) containing5% (by volume) VC. The cells were assembled in an argon-filled glove box with the concentrations of moisture and oxygen at less than1ppm. The galvanostatic charge/discharge cycling performance was measured using a LAND battery testing system in the voltage range from 5 mV to 3 V versus Li/Li^+. CV was performed using an IM6 electrochemical workstation between 5 mV and 3 V versus Li/Li^+ at a scan rate of 0.1 mV/s. Electrochemical impedance spectroscopy (EIS) was performed over frequencies ranging from 100 kHz to 100 mHz.

The preparation of full cells: All full cells were carried out in 2032 coin type cells. $LiMn_2O_4$ was used as the cathode and the graphdiyne film was used as the anode, which was separated by a Celgard 2500 polymeric separator with the cathode. The electrolyte comprised a solution of 1M LiPF6 in ethylene carbonate (EC)/dimethyl carbonate (DMC)/ diethyl carbonate (DEC) (1:1:1 by volume).

Materials characterization

The X-Ray photoelectron spectrometer (XPS) was collected on VG Scientific ESCALab220i-XL X-Ray photoelectron spectrometer, using Al Ka radiation as the excitation sources. The banding energies obtained in the XPS analysis were corrected with reference to C1s (284.8 eV). Raman spectra were recorded at room temperature using an NT-MDT NTEGRA Spectra system with excitation from an Ar laser at 473 nm. Morphological information was obtained using field emission scanning electron microscopy (FESEM, HITACHI S-4800). The GDY films were transferred to a copper screen and then the samples were characterized using TEM and HRTEM using a Hitachi-2010 apparatus. Nitrogen adsorption/desorption measurements were performed at 77 K using a Quantachrome Autosorb gas-sorption system.

Results and discussion

We attribute the excellent electrochemical performance of GDY to its high theoretical capacity, remarkable electrical conductivity, and excellent chemical stability. The direct preparation of GDY in high yield was a challenge until recently when Li *et al*. developed an in situ cross-coupling reaction on copper foil to fabricate a large-area ordered film of GDY from hexaethynylbenzene (Fig. 1-I and -II) [18,19]. In the present study, we use that method to synthesize three kinds of GDY films of various thicknesses on copper surfaces; we call these films GDY-1 (0.24 mg/cm^2), GDY-2 (0.48 mg/cm^2), and GDY-3 (0.72 mg/cm^2). Different thickness was achieved by changing the loading weight of hexakis[(trimethylsilyl)ethynyl]benzene. Both sides of the copper foil would be covered by GDY firstly. After the GDY was formed on the copper foil, we carefully scraped the GDY on one side. So the sample we used for test only have GDY left on one side of the copper foil. The details of the experiment were given in the supporting information. We use scanning electron microscopy (SEM) and transmission electron microscope (TEM) to investigate the morphology of GDY films.

The SEM images of GDY-1 under different degrees of magnification in Fig. 2a and b indicate that this film was uniform and continuous despite having some particles attached on the surface. The thickness of the GDY-1 film was approximately 10.9 μm (Fig. 2c). Fig. S1-2 in supporting formation showed that the thickness of the GDY-2 and GDY-3 films was about 22.1 and 30.9 μm, respectively. Fig. 2d displayed the TEM image of GDY-1 film. The cross-sectional high resolution TEM (HRTEM) image of GDY-1 was showed in Fig. 2e. The green line highlights the stacking layers of GDY. According to this HRTEM image, the layer-to-layer distance can be measured. As showed in Fig. 2e, the layer-to-layer distance was 0.365 nm, which is larger than that of graphite (0.335 nm). Same results were got on GDY-2 and GDY-3 films. The TEM/HRTEM images of GDY-2 and GDY-3 films can be found in the supporting information Figs. S3 and S4. The layer-to-layer distance of GDY-2 and GDY-3 is also 0.365 nm.

Raman spectroscopy was used to evaluate the quality and uniformity of the GDY films [18]. Similar to what has been observed previously, the Raman spectra of GDY-1 recorded at various positions on the film (Fig. 2d) reveal two prominent peaks: a D band at 1362.7 cm^{-1} and a G band at 1591.7 cm^{-1} [18].The peaks at 2190.1 cm^{-1} can be attributed to the vibration of conjugated diyne links ($-C\equiv C-C\equiv C-$) [18]. The intensity of the D band is strongly associated with structural defects,

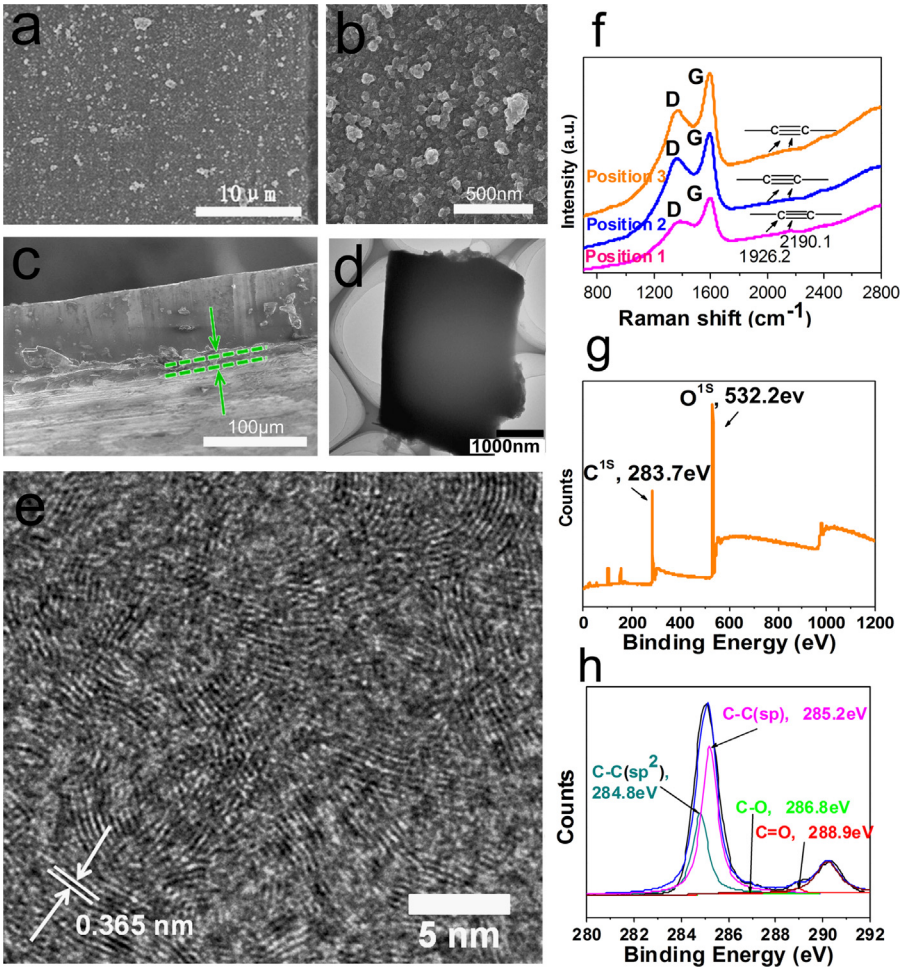

Fig. 2 Characterization of as-prepared GDY. (a)Top-view, (b) expanded view, (c) cross sectional SEM, (d) TEM and (e) cross-sectional HRTEM images of GDY-1. (f) Typical Raman spectra of GDY-1, recorded at three different points. (g) Survey and (h) C1s binding energy profiles of GDY-1 with fitting recorded using X-ray photoemission spectroscopy.

including disordered carbon atoms and edges; the G band corresponds to first-order scattering of the E_{2g} stretching vibration mode observed for sp^2-hybridized carbon atom domains in aromatic rings. For GDY-1, the ratio of the intensities of the D and G bands was 0.826, suggesting a GDY film possessing high order and low content of defects. As shown in Fig. S3, the ratio of the intensities of the D and G bands for GDY-2 and GDY-3 was 0.815 and 0.810, respectively, which indicates they are also high order and low content of defects.

X-ray photoelectron spectroscopy (XPS) was used to further characterize the GDY films and confirm unambiguously that these films are built exclusively from elemental carbon. In Fig. 2e and f, the C 1 s peak appears at 283.7 eV, similar to the binding energy of a C1 s orbital. After subtraction of the Shirley background, followed by fitting with a mixture function of Lorentzian and Gaussian, we could deconvolute the C 1 s peak into four mainly sub-peaks: at 284.8, 285.2, 286.8, and 288.9 eV. We assign these transitions to a C 1 s orbitals in C–C (sp^2), C–C (sp), C–O, and C=O bonds, respectively. The area ratio for the signals of the sp- and sp^2-hybridized carbon atoms in each as-prepared GDY film was 2, as would be predicted for a structure consisting of benzene rings linked together through diyne moieties. The presence of a signal for O1s at 533.2 eV arose from both the absorption of O_2 and dangling $-C\equiv CH$ bond oxidized by air when we exposed our GDY films to air. The fitting detail of O1 s spectra was showed in Fig. S5 (Supporting information). The fitting peak of C 1 s at 288.9 eV was attributed to C=O bonds, which further confirm the oxidization of dangling $-C\equiv CH$ bond.

We use a typical Li-ion battery to estimate the Li storage capacity of GDY (Fig. 1-III). Electrochemical experiments were performed using 2032 coin-type cells. We cut the GDY films grown on the copper foil into pieces and used them directly as working electrodes without the addition of any binders. A pure Li foil was used as the counter electrode. The counter electrode was separated from the working electrode by a Celgard 2500 polymeric separator. The electrolyte comprised a solution of 1M $LiPF_6$ in ethylene carbonate (EC) and dimethyl carbonate (DMC) (1:1, v/v) or a solution of 1M $LiPF_6$ in EC, DMC, and diethyl carbonate (DEC) (1:1:1, v/v/v) containing 5% (by volume) vinylene carbonate (VC). We assembled the cells in an argon-filled glove box in which the concentrations of moisture and oxygen were below 1ppm.

Our prepared Li-ion batteries incorporating GDY electrode exhibited excellent electrochemical performance. The SEM image in Fig. 3a reveals that the GDY-1 film essentially maintained its

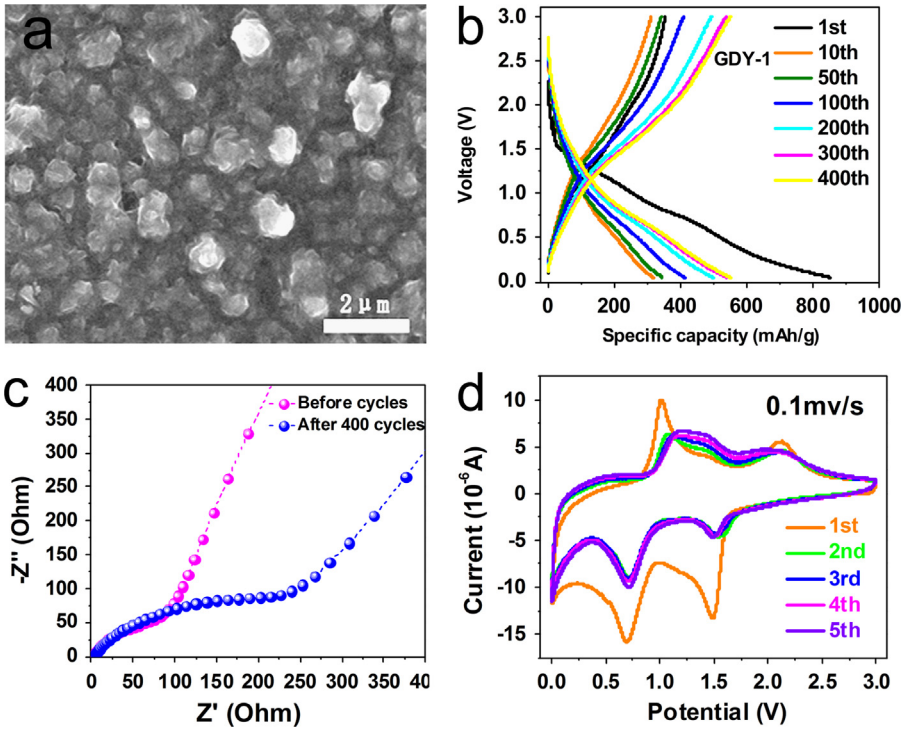

Fig. 3 Performance of GDY in a Li-ion half cell. (a) SEM image of a GDY-1 film after 400 cycles. (b) Galvanostatic charge/discharge profile of a GDY-1 electrode at a current density of 500 mA/g, recorded between 5 mV and 3 V. (c) Nyquist plots of a GDY-1-based electrode before and after 400 cycles at a current density of 500 mA/g. (d) Cyclic voltammetry curves of the GDY-1-based electrode with copper substrate, recorded at a scan rate of 0.1 mV/s.

initial morphology after 400 cycles, although the particle size had increased and some nanosheets had been generated around the particles; we suspect that these features were responsible for the increased capacity during cycling. The specific capacity of the GDY film increased continuously during the first 200 cycles (shown in Fig. 3b) and remained stable during the next 200 cycles. The initial coulombic efficiency was very low (41.7%), presumably because of the formation of a solid electrolyte interphase (SEI) layer on the surface of the GDY electrodes during the first discharge step.

Furthermore, from electrochemical impedance spectra of the GDY films before and after cycling, Nyquist plots (Fig. 3c) revealed that the diameter of the semicircle for the GDY-1 electrode after 400 cycles in the high-medium frequency region was much larger than that for the electrode prior to cycling, suggesting increased contact and charge-transfer resistances of the GDY-1 electrode. We attribute this enlargement to the increase in particle size during cycling. Two pairs of cathodic/anodic peaks were observed on GDY-1-based electrode (Fig. 3d). Further control experiments on copper foil and GDY scraped from the GDY film separately were done (Fig. S5), indicated that the two pairs of cathodic/anodic peaks were attributed to copper substrate. Because cyclic voltammetry experiments of GDY-1-based electrode was performed with its copper substrate. The cyclic voltammetry curve in Fig. 3d was resulted from both GDY-1 film and its copper substrate. Actually, GDY-1 has no clear reduction and oxidation peaks as shown in supporting information (Fig. S5b).

A highly efficient Li-ion battery requires its electrode materials to possess at least two qualities: (1) a high capacity for Li storage and (2) sufficient space for Li diffusion. The unique structure of GDY features a large number of nanoscale, triangular pores that endow GDY with a great number of Li storage sites and favors the absorption/desorption and diffusion of Li ions, both in-plane and out-of-plane. Calculations have suggested that Li atoms readily occupy three symmetric sites in the triangle-like pores, with a binding energy (2.17 eV) higher than those for absorption at the centre of the hexagons (1.56 eV) or at the centre of the triangle-like pores (2.04 eV) [25]. The key point is that the binding in three symmetric sites of the triangular pores is energetically the most favorable and stable. Based on this occupation pattern, the theoretical capacity can reach twice that of commercial graphite (as high as 744 mAh/g) [24]. The unique atomic arrangement and electronic structure enables the Li ions to diffuse readily on the GDY layers with moderate energy barriers ranging from 0.18 to 0.84 eV. With its considerably high Li ion mobility, high Li ion storage capacity, and high Li ion diffusion, GDY appears to be an efficient material for use in Li storage based energy application.

We evaluated the electrochemical performance of GDY samples of different film thicknesses through galvanostatic charge/discharge cycling in a cell using Li metal as the counter electrode at a high current density of 500 mA/g (Fig. 4a). The specific capacity of these GDY samples increased continuously within 400 cycles. Fig. 4b reveals that the capacity of the GDY-1-based electrode increased from 320 to 495 mAh/g during the first 200 cycles (cf. from 185 to 260 mAh/g for the GDY-2-based electrode; from 101 to 127 mAh/g for the GDY-3 based electrode), but remained stable at approximately 520 mAh/g (285 mAh/g for the GDY-2-based electrode, 136 mAh/g for the

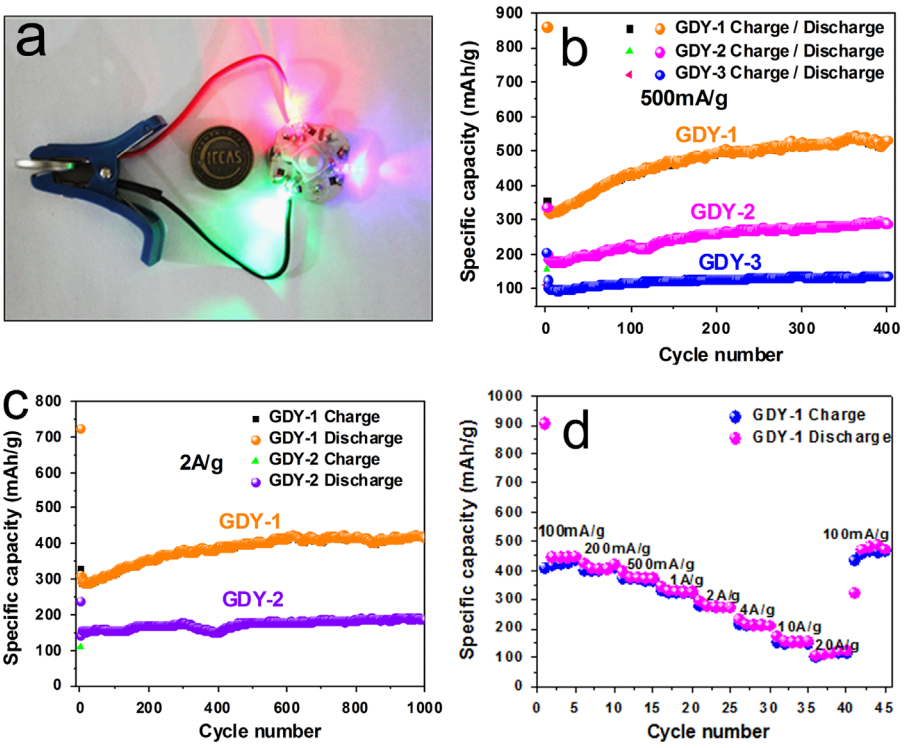

Fig. 4 Performance of GDY in a Li-ion cell. (a) Photograph exhibition of the assembled full Li-ion battery and applied discharge for the lighting of an LED bulb. (b) Cycle performance of the GDY-1, GDY-2, and GDY-3 electrodes at a current density of 500 mA/g between 5 mV and 3 V. (c) Cycle performance of the GDY-1 and GDY-2 electrodes at a current density of 2 A/g between 5 mV and 3 V. (d) Rate performance of the GDY-1 electrode. The results of b, c, and d were obtained by a half cell.

GDY-3-based electrode) during the next 200 cycles, close to the theoretical specific capacity of monolayer GDY (744 mAh/g). This behavior illustrates a gradual activation process initially with additional deflects generated upon charge/discharge cycling. The long cycle life of 400 cycles and even 1000 cycles can eliminate the effect of electrolyte decomposition, which could lead the assembled batteries disintegrated gradually and a short cycle life. The initial coulombic efficiencies for the GDY-1-, GDY-2-, and GDY-3-based electrodes were, however, very low, at 41.7, 47.0, and 52.2%, respectively. The origin of the low coulombic efficiencies is likely due to the formation of SEI layers on the surfaces of the GDY electrodes during the first discharge step.

In the GDY structure, each benzene ring is connected to six adjacent benzene rings through two carbon-carbon triple bonds, resulting in a flat porous structure exhibiting high chemical stability and electrical conductivity. These triple bonds open up a potentially limitless array of geometries, which provide a big surface area. GDYs possess a band gap [22,27] which display distinct electronic properties. The advantages of this material have attracted great interest as better candidate material for application in Li-ion batteries and development of modern macro- and nano-electronics. Most interestingly, the cells containing GDY-based electrodes displayed extremely long cycle lives. We obtained reversible capacities for the GDY-1 and GDY-2 electrodes of up to 420 and 192 mAh/g, respectively, after 1000 cycles at a high current density of 2 A/g (Fig. 4c). We ascribe the excellent rate capacities and superior cycle stabilities to the high conductivity and chemical stability of GDY. Fig.4d displays the results from our further study of the rate performance of GDY-1; we could still observe reversible capacities of 231, 173, and 121 mAh/g at high current densities of 4, 10, and 20 A/g, respectively. We used the GDY films, grown on copper as the current collector, directly as working electrodes without adding any binders; this approach is conductive to the rapid transfer of electrons. After 200 cycles, the capacity of GDY-1 could reach 612 (Fig. S13a), 584 (Fig. S13b) and 465 (Fig. S13d) mAh/g at current densities of 100, 200, 1000 mA/g, respectively. Based on the results described above, the assembled Li-ion batteries with GDY-based electrode exhibited excellent electrochemical performance, including high specific capacities, outstanding rate performance, and superior long cycle lives, which we ascribe to the high theoretical specific capacity, superior electrical conductivity, and excellent chemical stability of GDY.

Graphite is used as the major commercially available anode in Li-ion batteries for its better cycle performance and low cost, but its theoretical specific energy capacity is only 372 mAh/g [6], which currently can't satisfy the increasing demand of high capacity. In terms of capacity, the theoretical specific energy capacity of Si based is Li-Ion battery is 4200 mAh/g, more than 10 times higher than that of the current graphite anode; about 3500 mAh/g is accessible during electrochemical lithiation [28-31]. However, Si-based electrodes typically suffer from poor capacity retention due to its volume expansion issue (about 300%). So lots of Si based structures, such as Si/C composite, Nanostructured Si, and so on, have been developed to address these challenges, those of which undoubtedly increased the cost of battery. Considering the directly applying materials in battery, pristine graphene-based electrodes showed the same theoretical specific energy capacity as GDY. But the longest cycle lives obtained for

pristine graphene-based Li-ion batteries were ranged from 100 to 130, with very low initial coulombic efficiencies (ca. 20–30%). [15,32–34] Preparing graphene with large quantity and good quality under acceptable cost is still current effort target. The GDY could be synthesized through conventional chemical reaction, which means the cost could be decreased after improving the synthesis process. Therefore, compared with graphite, graphene and silicon, the electrochemical properties of GDY including good capacity, long cycle life and outstanding rate capacity indicate that GDY can be another promising electrode material.

The Li atom storage in multilayer GDY could be occurred in two ways as interlayer insertion/extraction (Fig. 5a) and surface absorption/desorption process (Fig. 5b). The interlayer insertion/extraction method of Li storage in multilayer GDY corresponded to a Li storage capacity of LiC_6. Due to the flat carbon (sp2 and sp) network endows the GDY material with uniformly distributed pores, as displayed in Fig. 5b, there are three possible sites for Li atom absorption on GDY: one Li atom above the center of a benzene ring (Fig. 5b-I), corresponding to a Li storage capacity of LiC_{18}; one Li atom above the center of a triangle-like pore(Fig. 5b-II), corresponding to a Li storage capacity of LiC_9; three Li atoms above the center of triangle-like pores(Fig. 5b-III), absorbed on both sides of surface (Fig. 5c and d), corresponding to a Li storage capacity of LiC_6; and three Li atoms above the center of triangle-like pores(Fig. 5b-III), absorbed on one sides of surface (Fig. 5e and f), corresponding to a Li storage capacity of LiC_3. Theoretical calculations predict that the structure in Fig. 5b-III is the dominant mode of Li absorption on GDY. Therefore, we wished to investigate and reveal the method of Li storage in multilayer GDY directly from our experiments. According to a previous calculations [22], the theoretical mass density of monolayer GDY is 0.46 mg/m^2. To compare our experimental data with the theoretical value, here we define the surface capacity C_s (mAh/cm^2) as

$$C_s = \frac{C}{S} \quad (1)$$

Where C is the specific capacity (mAh/g) and S is the specific surface area (m^2/g) of sample.

The theoretical capacity of monolayer GDY (Fig. 5b-III Fig. 5e) is 744 mAh/g. As a result, the theoretical surface capacities of GDY are 1.71×10^{-5} mAh/cm^2 for interlayer insertion/extraction, 0.58×10^{-5} mAh/cm^2 for the structure in Fig. 5b-I, 1.14×10^{-5} mAh/cm^2 for the structure in Fig. 5b-II, and 3.42×10^{-5} mAh/cm^2 for the structure in Fig. 5b-III. Nitrogen absorption/desorption measurements revealed that the specific surface areas of GDY-1 and GDY-2 were 1329 and 654 m^2/g, respectively. Through formula (1), we transformed the specific capacities of GDY-1 and GDY-2 into values of 3.91×10^{-5} mAh/cm^2 (520 mAh/g) and 4.36×10^{-5} mAh/cm^2 (285 mAh/g), respectively. Those two values are bigger than the theoretical surface capacities 3.42×10^{-5} mAh/cm^{2}of GDY. Normally, theoretical capacity was always obtained under small charge/discharge rate. Here, even at a large current density like 500 mA/g, the surface capacities values are still larger than the theoretical capacity of monolayer GDY in Fig. 5a-III, which should be due to the Li intercalation into GDY layers rather than merely absorption on the surface. According to the previous reports and the differential voltage curves (Fig. S12 in supporting information) [35,36], the specific capacity below 0.4 V corresponds to the Li intercalation into GDY layers; the specific capacity above 0.4 V is associated with Li absorption on the GDY surface or on the edge plane. [37,38] Therefore, the absorption capacity of GDY-1 and GDY-2 are 2.99×10^{-5} mAh/cm^2 (398 mAh/g, above 0.4 V) and 3.03×10^{-5} mAh/cm^2 (198 mAh/g, above 0.4 V), respectively. These values are larger than the theoretical capacity of monolayer GDY in Fig. 5b-I (is $0.58 \times 10^{-}$

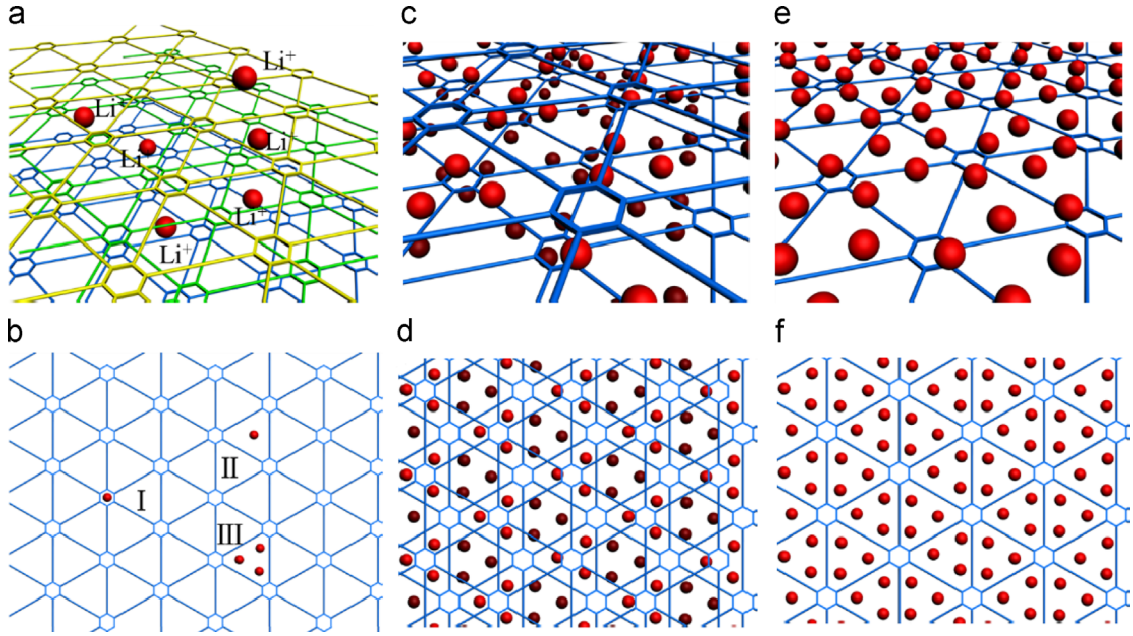

Fig. 5 Li-Storage of GDY in a Li-ion cell. (a) Li-intercalated GDY. (b) Three different sites for occupation by Li atoms in GDY. Absorption of Li atoms on (c, d) both sides and (e, f) one side of a GDY plane; and (c, e) angled and (d, f) top views of Li absorption geometries.

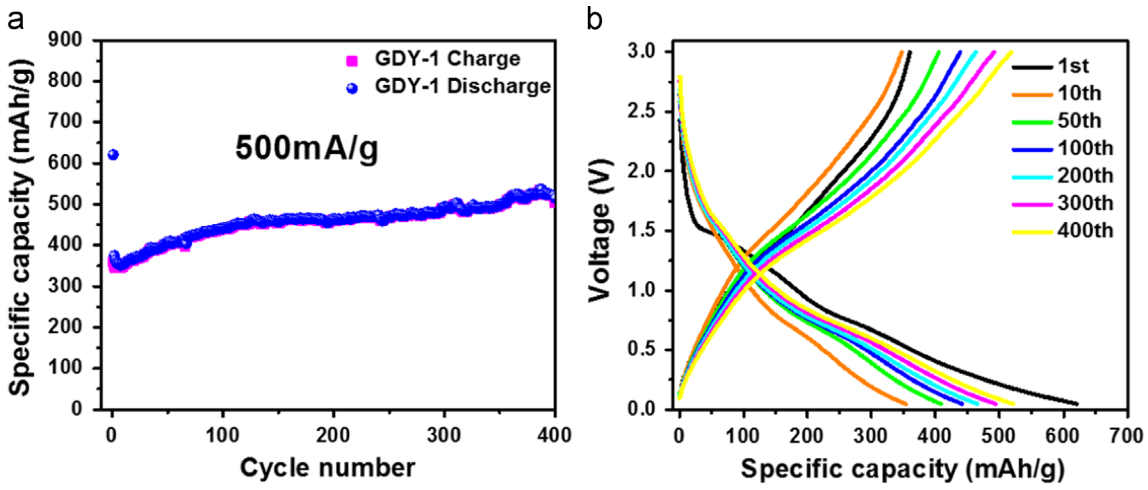

Fig. 6 Control performance of GDY in a Li-ion cell. (a) Cycle performance and (b) galvanostatic charge/discharge profiles of the GDY-1 electrode at a current density of 2 A/g between 5 mV and 3 V in an electrolyte of 1M LiPF6 in EC/DMC/DEC (1:1:1, v/v/v) containing5% (by volume) VC.

^{5}mAh/cm^2) and 5b-II (is 0.58×10^{-5} mAh/cm^2), but smaller than the theoretical capacity of monolayer GDY in Fig. 5b-III. Those results indicated that Li absorption on GDY is mainly consistent with method showed in Fig. 5b-III (is 3.42×10^{-5} mAh/cm^2). So Li storage in multilayer GDY occurs mainly through both interlayer insertion/extraction way (Fig. 5a) and surface absorption/desorption method on the surface of the GDY films (Fig. 5c and d). The inaccuracy of nitrogen absorption/desorption measurements would result in difference between measured specific surface areas and theoretical value of the specific surface areas. So further study is still need to further understand the mechanism, such as HRTEM and spherical aberration-corrected electron microscope to directly investigate the Li atom in GDY layer.

To improve the cycle stability of GDY, we tested the behavior of a different electrolyte, 1M $LiPF_6$ in EC/DMC/DEC (1:1:1, v/v/v) containing 5% (by volume) VC, under the same electrochemical conditions. By adding VC, an effective SEI forming additive, the cycle stability of GDY-based electrode improved as shown in Fig. 6. In addition, we obtained a similar result, with a high capacity (525 mAh/g) achieved after 400 cycles at a current density of 500 mA/g (Fig. 6). Nevertheless, there remained a large amount of irreversible capacity; definite interpretation of this behavior will require further investigation.

Conclusions

In summary, we have synthesized three different large-area GDY films of controlled thickness, and applied them as electrode materials for Li-ion batteries to estimate the Li storage capacity. We found that the assembled GDY-based Li-ion batteries exhibited excellent electrochemical performance, including high specific capacities, outstanding rate performances, and long cycle lives. In addition, the Li storage in multilayer GDY occurs primarily through the interlayer insertion/extraction and surface absorption/desorption methods. The unique structure of GDY, with its numerous large triangle-like pores, endows it with many Li storage sites and facilitates the rapid transport of electrons and ions. We hope that designing and preparing novel carbon-based materials with large pores will open up new approaches for the development of Li storage materials exhibiting high capacities and excellent cycling stabilities, thereby satisfying the future requirements of next-generation Li storage batteries.

Acknowledgments

This study was supported by the “100 Talents” program of the Chinese Academy of Sciences, the National Natural Science Foundation of China Youth Science Fund Project (21301184), the National Basic Research 973 Program of China (2011CB932302 and 2012CB932900) and the National Nature Science Foundation of China (201031006, 91227113 and 21290190).

Appendix A. Supporting information

Supplementary data associated with this article can be found in the online version at http://dx.doi.org/10.1016/j.nanoen.2014.11.036.

References

[1] V. Etacheri, R. Marom, R. Elazari, G. Salitra, D. Aurbach, Energ. Environ. Sci. 4 (2011) 3243–3262.
[2] S. Flandrois, B. Simon, Carbon 37 (1999) 165–180.
[3] B. Kang, G. Ceder, Nature 458 (2009) 190–193.
[4] I. Lahiri, W. Choi, Crit. Rev. Solid State 38 (2013) 128–166.
[5] J.M. Tarascon, M. Armand, Nature 414 (2001) 359–367.
[6] V. Manev, I. Naidenov, B. Puresheva, P. Zlatilova, G. Pistoia, J. Power Sources 55 (1995) 211–215.
[7] R.O. Loutfy, S. Katagiri, Perspectives of Fullerene, in: E. Osawa (Ed.), Nanotechnology, Kluwer Academic Publishers, Dordrecht, 2002, pp. 357–367.
[8] D.V. Nicolau, Nanotechnology 16 (2005) 488–494.
[9] M.S. Dresselhaus, G. Dresselhaus, P.C. Eklund, Science of Fullerenes and Carbon Nanotubes: their Properties and Applications, Academic Press, Inc., San Diego, 1996.

[10] E. Frackowiak, S. Gautier, H. Gaucher, S. Bonnamy, F. Beguin, Carbon 37 (1999) 61–69.
[11] B.J. Landi, M.J. Ganter, C.D. Cress, R.A. DiLeo, R.P. Raffaelle, Energ. Environ. Sci. 2 (2009) 638–654.
[12] S.W. Lee, N. Yabuuchi, B.M. Gallant, S. Chen, B.-S. Kim, P.T. Hammond, Y. Shao-Horn, Nat. Nanotech 5 (2010) 531–537.
[13] H. Shimoda, B. Gao, X.P. Tang, A. Kleinhammes, L. Fleming, Y. Wu, O. Zhou, Phys. Rev. Lett. 88 (2002) 015502.
[14] K.S. Novoselov, V.I. Falko, L. Colombo, P.R. Gellert, M.G. Schwab, K. Kim, Nature 490 (2012) 192–200.
[15] T. Bhardwaj, A. Antic, B. Pavan, V. Barone, B.D. Fahlman, J. Am. Chem. Soc. 132 (2010) 12556–12558.
[16] B.Z. Jang, C. Liu, D. Neff, Z. Yu, M.C. Wang, W. Xiong, A. Zhang, Nano Lett. 11 (2011) 3785–3791.
[17] G. Profeta, M. Calandra, F. Mauri, Nat. Phys 8 (2012) 131–134.
[18] G. Li, Y. Li, H. Liu, Y. Guo, Y. Li, D. Zhu, Chem. Commun. 46 (2010) 3256–3258.
[19] Y. Li, L. Xu, H. Liu, Y. Li, Chem. Soc. Rev. 43 (2014) 2572–2586.
[20] J. Zhong, J. Wang, J.G. Zhou, B.H. Mao, C.H. Liu, H.B. Liu, Y.L. Li, T.K. Sham, X.H. Sun, S.D. Wang, J. Phys. Chem. C 117 (2013) 5931–5936.
[21] B. Jang, J. Koo, M. Park, H. Lee, J. Nam, Y. Kwon, H. Lee, Appl. Phys. Lett. 103 (2013) 63904.
[22] M. Long, L. Tang, D. Wang, Y. Li, Z. Shuai, ACS Nano 5 (2011) 2593–2600.
[23] K. Srinivasu, S.K. Ghosh, J. Phys. Chem. C 116 (2012) 5951–5956.
[24] C. Sun, D.J. Searles, J. Phys. Chem. C 116 (2012) 26222–26226.
[25] H. Zhang, Y. Xia, H. Bu, X. Wang, M. Zhang, Y. Luo, M. Zhao, J. Appl. Phys. 113 (2013) 044309.
[26] Q. Tang, Z. Zhou, Z. Chen, Nanoscale 5 (2013) 4541–4583.
[27] G.F. Luo, X.M. Qian, H.B. Liu, R. Qin, J. Zhou, L.Z. Li, Z.X. Gao, E.G. Wang, W.-N. Mei, J. Lu, Y.L. Li, S. Nagase, Phys. Rev. B 84 (2011) 075439.
[28] N. Liu, Z. Lu, J. Zhao, M.T. McDowell, H.W. Lee, W. Zhao, Y. Cui, Nat. Nanotech 9 (2014) 187–192.
[29] M.T. McDowell, S.W. Lee, W.D. Nix, Y. Cui, Adv. Mater. 25 (2013) 4966–4984.
[30] B.A. Boukamp, G.C. Lesh, R.A. Huggins, J. Electrochem. Soc. 128 (1981) 725–729.
[31] J. Li, J.R. Dahn, J. Electrochem. Soc 154 (2007) A156-A161.
[32] P. Lian, X. Zhu, S. Liang, Z. Li, W. Yang, H. Wang, Electro-chim. Acta 55 (2010) 3909–3914.
[33] O.A. Vargas, C, A. Caballero, J. Morales, Nanoscale 4 (2012) 2083–2092.
[34] G. Wang, X. Shen, J. Yao, J. Park, Carbon (2009) 2049-2053.
[35] J. Hu, H. Li, X. Huang, Solid State Ionics 178 (2007) 265–271.
[36] E. Yoo, J. Kim, E. Hosono, H.-s. Zhou, T. Kudo, I. Honma, Nano Lett. 8 (2008) 2277–2282.
[37] R. Yazami, M. Deschamps, J. Power Sources 54 (1995) 411–415.
[38] G. Wang, X. Shen, J. Yao, J. Park, Carbon 47 (2009) 2049–2053.

Changshui Huang received his BS from University of Science and Technology of China (2003) and PhD from Institute of Chemistry, the Chinese Academy of Sciences (ICCAS) (2008). After that he worked in ICCAS. During 2010 to 2014 he conducted his postdoc research in University of Wisconsin-Madison. Currently he works at Qingdao Institute of Bioenergy and Bioprocess Technology and ICCAS. His research interesting expanding the application of carbon-based nano materials to develop novel model energy storage device and related key materials.

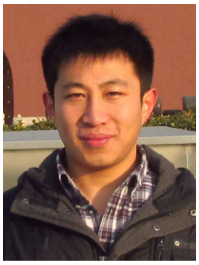

Shengliang Zhang received his Bachelor's in 2011 from Qingdao University of Science and Technology. He joined the Qingdao Institute of Bioenergy and Bioprocess Technology, Chinese Academy of Sciences for Master study. His current research focuses on carbon-based materials for lithium/sodium ion batteries.

Huibiao Liu received his PhD degree in Inorganic Chemistry in 2001 at Nanjing University. He is currently a professor in Prof. Yuliang Li's group, the Institute of Chemistry, Chinese Academy of Sciences. His research interests in the fields of fabrications and properties of inorganic/organic hybrid and conjugated organic molecular nanostructures, development of novel methods for tuning the structures and properties.

Yongjun Li was born in 1975 in Sichuan, China. He received his Master degree in Chemistry from Sichuan University in 2001, and he earned his Ph.D. in organic chemistry in 2006 at ICCAS. He is currently an associate professor in Prof. Yuliang Li's group, ICCAS, working on the design and synthesis of functional organic molecules.

Guanglei Cui received his PhD from ICCAS (2005). From 2005 to 2009, he had worked at Max-Planck-Institute for Polymer Research and Solid State research as a postdoctoral scientist on Ener. Chem. Project. Then he joined in the QIBEBT as professor from 2009. His research interests include low-cost and highly efficient energy-storage materials, electrode materials, and novel energy devices including lithium ion batteries, super-capacitors, and perovskite solar cells.

Yuliang Li is a professor at the Institute of Chemistry, Chinese Academy of Sciences. His research interests lie in the fields on design and synthesis of functional molecules, self-assembly methodologies of low dimension and large size molecular aggregations structures, chemistry of carbon and rich carbon, with particular focus on the design and synthesis of photo-, electro-active molecular heterojunction materials, and nanoscale and nano-structural materials.